

Kabseog Kim · Jeong-Bong Lee

## High aspect ratio tapered hollow metallic microneedle arrays with microfluidic interconnector

Received: 31 August 2005 / Accepted: 26 October 2005 / Published online: 11 July 2006  
© Springer-Verlag 2006

**Abstract** We present a novel microfabrication method for a tapered hollow metallic microneedle array and its complete microfluidic packaging for drug delivery and body fluid sampling applications. Backside exposure of SU-8 through a UV transparent substrate was investigated as a means of fabricating a dense array of tall (up to 400  $\mu\text{m}$ ) uniformly tapered SU-8 pillar structures with angles in the range of 3.1–5° on top of the SU-8 mesa. Conformal electroplating of metals on top of the array of the tapered SU-8 pillars, lapping of the tip of the metallic microneedles with planarizing polymer, and removal of the SU-8 sacrificial layers resulted in an array of tapered hollow metallic microneedles with a fluidic reservoir on the backside. A microfluidic interconnector assembly was designed and fabricated using SU-8 and conventionally machined PMMA in a way that it has a male interconnector, which directly fits into the fluidic reservoir of the microneedle array at one end and the other male interconnector, which provides fluidic interconnection to external devices at the other end. The fluid flow rate was measured and it showed 0.69  $\mu\text{L/s}$ . per microneedle when the pressure of 6.89 KPa (1 psi) was applied.

using conventional hypodermic syringes is due to the fact that the needle is large and penetrates deep into the skin with excessive contact with these sensory fibers in the cutaneous nerves. These sensory fibers and blood vessels reach to the dermis layer (50–150  $\mu\text{m}$  deep from the surface) of the skin. With the advances of micromachining technology, it is possible to make microneedles which are long enough to penetrate the epidermis but short enough not to penetrate deep into the dermis layer and further down in the subcutaneous tissue for minimally invasive transdermal drug delivery and body fluid sampling.

Recently, there have been many investigations on the development of various microneedles with a goal of realizing a safer and minimally invasive transdermal drug delivery device. Various materials such as silicon (Henry et al. 1998; Stoeber et al. 2005; Griss et al. 2003; Gardeniers et al. 2003), metal (McAllister et al. 1999; Davis et al. 2003; Kim et al. 2004), and polymer (Moon et al. 2005) have been studied as microneedle materials and various micromachining techniques including dry etch techniques (Henry et al. 1998; Stoeber et al. 2005; Griss et al. 2003), a combination of dry/wet etch techniques (Gardeniers et al. 2003), electroplating techniques (McAllister et al. 1999; Davis et al. 2003; Kim et al. 2004), and LIGA technique (Moon et al. 2005) have been used.

Microneedles and microneedle arrays can be used as stand-alone devices as well as parts of a more complicated biological detection/delivery system. Zimmermann et al. (2004) demonstrated a disposable self-calibrating continuous glucose monitor using hollow microneedles with a porous poly-Si dialysis membrane and enzyme-based flow-through sensor. Ahn et al. (2004) demonstrated a point-of-care clinical diagnostic system using multiple stacks of disposable functional plastic biochips with microneedles as body fluid sampling devices.

This paper is based on our previous work (Kim et al. 2004) and presents a relatively simple way to provide microfluidic interconnection to the metallic microneedle array using SU-8 and PMMA for the massively

### 1 Introduction

Sensory fibers in the cutaneous nerves detect external stimuli such as pain, temperature, and pressure, and generate signals which are relayed through a nerve pathway to the brain. The pain associated with injection

---

K. Kim (✉) · J.-B. Lee  
Erik Jonsson School of Engineering and Computer Science,  
The University of Texas at Dallas, Richardson, TX 75083, USA  
E-mail: kabseog@gmail.com

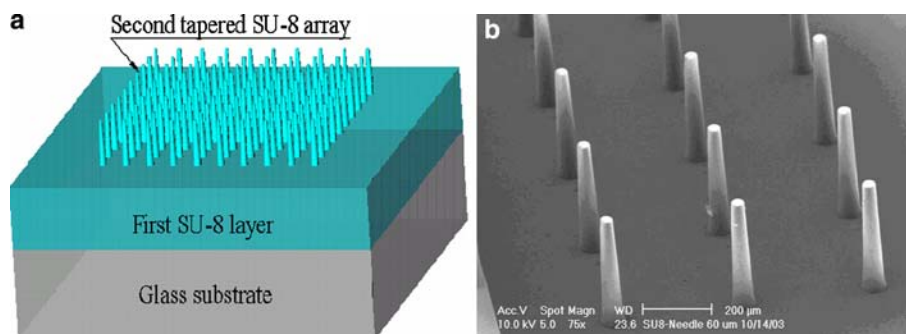
K. Kim  
HTMicro Analytical Inc., 3817 Academy Parkway S. NE,  
Albuquerque, NM, USA

produced metallic microneedle array using a modified SU-8—based UV-LIGA process. A complete testing on the flow rate of the microneedle array is also presented.

## 2 Fabrication of tapered metallic microneedle arrays

SU-8-based UV-LIGA processes have commonly been used to create very thick, high aspect ratio polymeric and metallic microstructures for various applications (Lorenz et al. 1997, 1998; Zhang et al. 2001). Recently, Peterman et al. (2003) suggested a backside exposure of thick SU-8 through a mask defined on a glass substrate to create a reentrant SU-8 structure for easy metallic mold production. In this study, exposure dose non-uniformity along the thickness of the thick resist was used to fabricate tapered pillar structures in SU-8. Further, such a tapered pillar array would be used as a sacrificial polymeric template to build final metallic structures, which would have a sharp tapered hollow shape. The fabrication was started with a spin-coating of an SU-8 release layer on top of a 3-inch diameter, 700  $\mu\text{m}$  thick Pyrex 7740<sup>®</sup> glass substrate and baked at 200°C for 90 s on a hotplate. A 200  $\mu\text{m}$  thick SU-8 2075 layer was spin-coated and was left on a flat surface for an hour for stress relaxation and planarization. The SU-8 was then soft-baked at 65°C for 5 min and at 95°C for 45 min on a hotplate. UV exposure was carried out with a dose of 1,000  $\text{mJ}/\text{cm}^2$  using a large square patterned (3 mm $\times$ 3 mm) mask. Next, a post-exposure bake was performed at 65°C for 1 min and 95°C for 15 min. Another 200  $\mu\text{m}$  thick layer of SU-8 was spin-coated on top of the post-exposure-baked first SU-8 layer. The double-layered SU-8 was soft-baked and exposed to the UV light with a circular array geometry mask with exposure doses of approximately 1,500  $\text{mJ}/\text{cm}^2$  for 200  $\mu\text{m}$  SU-8 pillars and 2,500  $\text{mJ}/\text{cm}^2$  for 400  $\mu\text{m}$  pillars. The samples were then developed in a SU-8 developer, PGMEA, for approximately 90 min and cleaned in oxygen plasma (200 W, 100% O<sub>2</sub>) for about 2 min utilizing a reactive ion etcher. Figure 1a shows a 3-D schematic diagram of the concept of the device and Fig. 1b shows an SEM photomicrograph of array of 400  $\mu\text{m}$  tapered SU-8 pillars which was patterned with the UV dose of 2,500  $\text{mJ}/\text{cm}^2$ .

**Fig. 1** A general view of **a** the fabricated double-layered SU-8 on a glass substrate and **b** SEM photomicrographs of 400  $\mu\text{m}$  pillar arrays at the UV dose of 2,500  $\text{mJ}/\text{cm}^2$



Based on the double-layered SU-8 backside exposure results, tapered hollow metallic microneedle arrays were massively fabricated. Figure 2 shows a series of SEM photomicrographs of the tapered hollow metallic microneedle array under fabrication. A double-layer (100 Å chromium and 1,000 Å copper) of electroplating seed was conformally deposited on top of the patterned double-layered 400  $\mu\text{m}$  SU-8 pillar array structures (Fig. 2a). Nickel electroplating was carried out using a nickel sulfamate bath at 55°C with a current density of 5  $\text{mA}/\text{cm}^2$  (Fig. 2b). In order to open the tips of the metallic microneedle array, an additional 450  $\mu\text{m}$  thick SU-8 layer was blanket deposited to provide an organic planarizing layer. The SU-8 layer was soft-baked for a longer time than the standard soft baking time and mechanically polished until the microneedle tips were opened (Fig. 2c). Then the unexposed planarizing SU-8 layer was removed by dipping in a developer. Next, the SU-8 release layer was stripped off, resulting in the separation of electrodeposited nickel coated double-layered SU-8 pillar structures from the glass substrate (Fig. 2d). Finally, the double-layered SU-8 pillar structures were dry-etched using O<sub>2</sub>/CF<sub>4</sub> (80%:20%) plasma with a power of 500 W in a TePla 300 microwave plasma etch system (TePla America, Inc., Hurst, TX, USA). It was followed by a wet-etch of the electroplating seed layers, resulting in a tapered hollow metallic microneedle array with a fluidic reservoir on the backside. The metallic wall thickness for the 200  $\mu\text{m}$  tall microneedle is 10  $\mu\text{m}$  and that for the 400  $\mu\text{m}$  tall microneedle is 20  $\mu\text{m}$ . Figure 3a shows the SEM photomicrograph of a 400  $\mu\text{m}$  tall microneedle array with a conventional gauge 28 stainless steel needle and Fig. 3b shows the backside of the hollow microneedle array which shows a fluidic reservoir and fluidic channels defined by complete removal of SU-8.

## 3 Microfluidic packaging for the microneedle array

In order to interface the small-scale microneedle array with macroscopic fluidic control devices such as pumps, valves, tubing, etc., a method of a microfluidic packaging for the tapered hollow metallic microneedle array with a fluidic reservoir was developed. A microfluidic

**Fig. 2** SEM photomicrographs of a microneedle array under fabrication: **a** 400  $\mu\text{m}$  tall tapered SU-8 pillar; **b** electroplated nickel covered SU-8 pillar; **c** an opened microneedle tip after SU-8 planarization and polishing; **d** 400  $\mu\text{m}$  tall metallic hollow microneedle array with 20  $\mu\text{m}$  in wall thickness

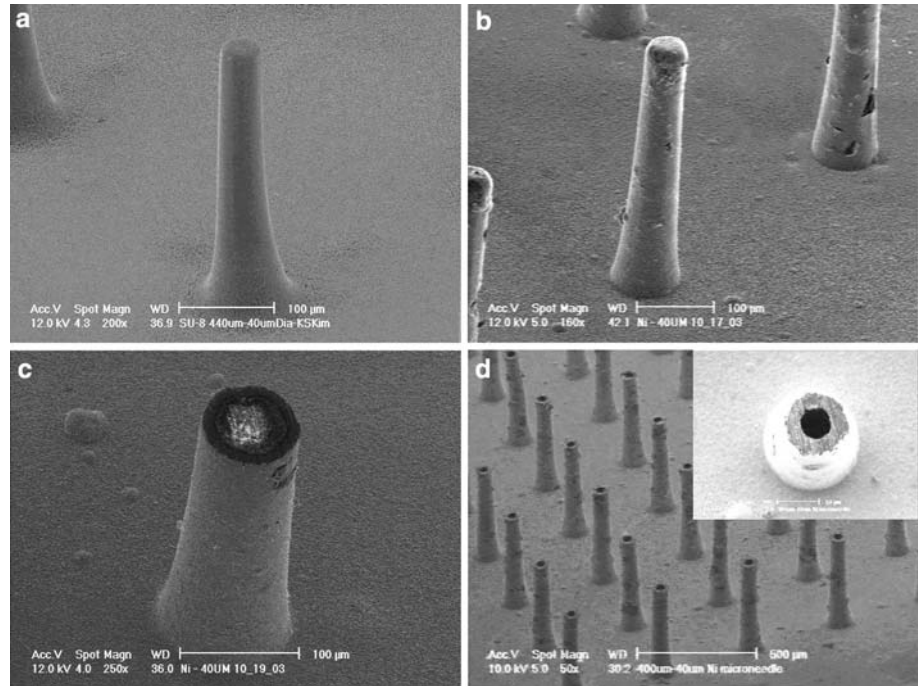
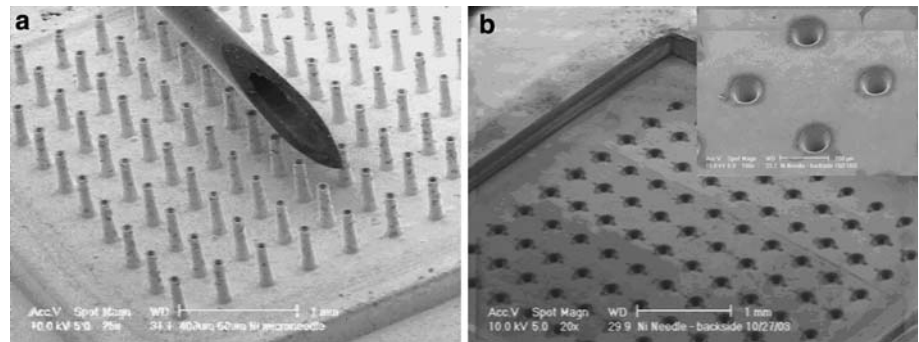


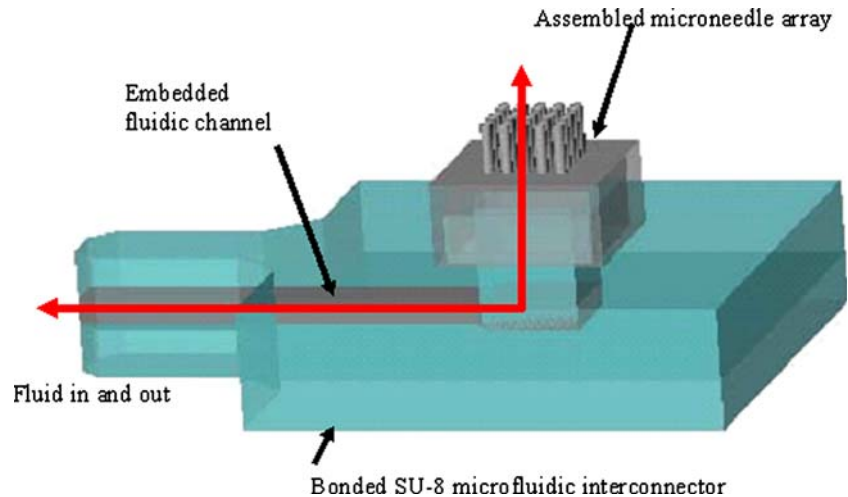
**Fig. 3** SEM photomicrographs of a microneedle array: **a** 400  $\mu\text{m}$  tall tapered hollow metallic microneedle array in comparison with a conventional gauge 28 stainless steel needle; **b** backside of the microneedle array which shows a fluidic reservoir and fluidic channels (through holes)



interconnector assembly was designed in a way that it has a male interconnector which directly fits into the fluidic reservoir of the microneedle array at one end and

the other male interconnector part which provides external fluidic interconnection to external tubing at the other end. Figures 4 and 5 show a conceptual diagram

**Fig. 4** A schematic diagram of a microfluidic packaging for the microneedle array



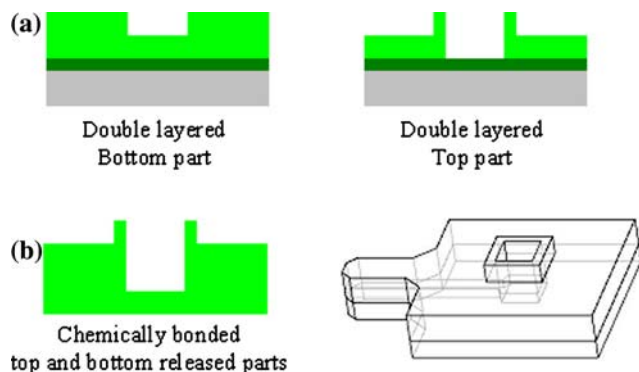


Fig. 5 Process flow for the microfluidic interconnector assembly fabrication

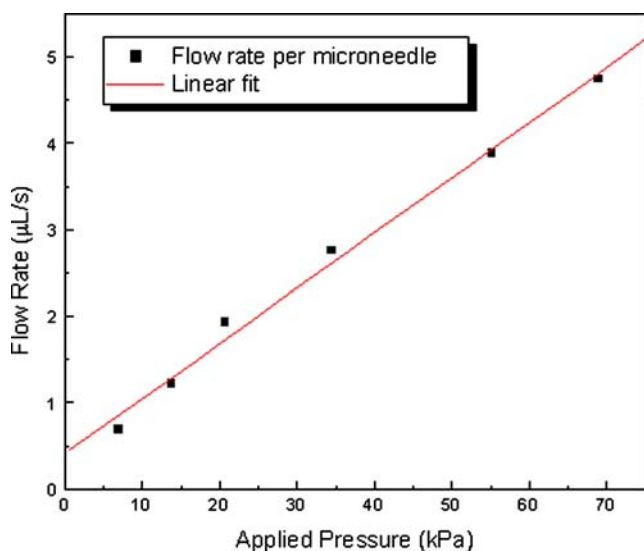


Fig. 6 Flow rate as a function of the applied pressure

and process sequence for such a microfluidic interconnector assembly.

Based on the optimized SU-8 process, two double-layered SU-8 microfluidic parts were fabricated separately on oxidized ( $1\ \mu\text{m}$  thick  $\text{SiO}_2$ ) silicon substrates as shown in Fig. 5a. After hard-bake of the SU-8 structures at  $150^\circ\text{C}$  for 1 h in an oven, both SU-8 fluidic parts were released from the silicon substrates by wet etching the  $\text{SiO}_2$  sacrificial layer in a buffered HF solution. The released fluidic parts were then chemically bonded to each other resulting in a microfluidic interconnector assembly with a microfluidic channel embedded in it (Fig. 5b). Finally, the microfluidic reservoir of the hollow metallic microneedle array was assembled onto the male interconnector at one end and the assembled area was chemically sealed (Fig. 5c). In order to ensure a leak-free bonding, additional epoxy was applied to the gap between the SU-8 fluidic interconnector and the metallic microneedle array.

#### 4 Fluid flow rate measurement

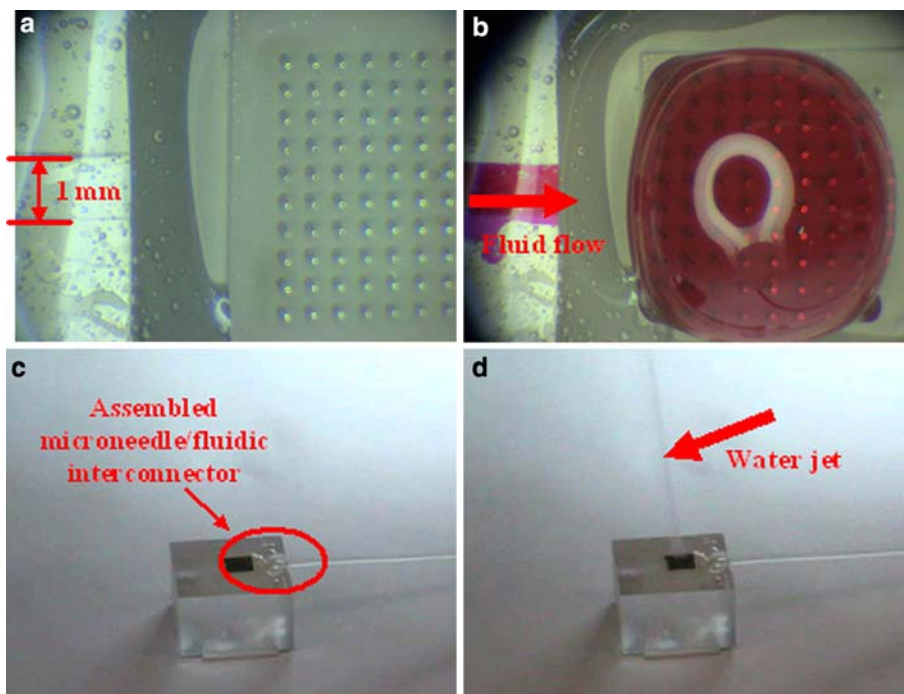
The assembled microneedle/microfluidic interconnector was bonded onto a conventionally machined PMMA master pad for easy handling. The male microfluidic interconnector in the packaged microneedle array was connected to a macroscopic external fluid reservoir via a  $1/16''$  (1.588 mm) inner diameter tube. A nitrogen tank was connected to the other end of the external reservoir. Three milliliters of DI water as a fluid medium was placed in the external fluid reservoir for each flow rate measurement test. The amount of time to empty the external fluid reservoir by applying a constant pressure ranging from 6.897 kPa (1 psi) to 68.97 kPa (10 psi) was recorded to calculate the flow rate corresponding to each pressure value. Figure 6 shows the relation between the applied pressure and the resulting flow rate of the assembled microneedle/microfluidic interconnector. The flow rate is linearly dependent on the applied pressure. There was no structural failure of the chemically bonded microfluidic packaging for the microneedle array with the applied pressure up to 68.97 kPa.

Figure 7a and b show the top view of the microfluidic interconnector before and after the fluid flow rate measurement test at the applied pressure of 6.897 kPa. The red-color dyed deionized water solution was gradually flowing out of the microneedle. As the applied pressure increased up to 68.97 kPa, strong water jets are coming out through hollow microneedles as seen in Fig. 7d.

#### 5 Conclusion

A simple and straightforward method of fabricating a microneedle array for drug delivery and body fluid sampling applications has been investigated. A 10 by 10, tapered hollow metallic microneedle array with a fluidic reservoir was built by using a novel microfabrication method. Both  $200\ \mu\text{m}$  tall and  $400\ \mu\text{m}$  tall metallic hollow microneedles with tapering angles less than  $5^\circ$  were realized. A multi-layered SU-8 microfluidic interconnector assembly was also fabricated and assembled with the microneedle array in order to interface the small-scale microneedle array with macroscopic fluidic control devices and systems. Using DI water as a fluidic medium, flow rates at different applied pressures were measured. It was concluded that the packaged microneedle array is capable of delivering liquid in a controlled manner. Since this overall process is relatively simple and rapid, it could be used for mass manufacturing of disposable metallic hollow microneedle arrays for painless transdermal drug delivery and body fluid sampling. Further development of microneedles using biocompatible materials and fully-included on-demand fluidic actuation systems is being carried out for generic biomedical applications.

**Fig. 7** Optical micrographs of the flow rate measurement test with varying input pressures: **a**  $P_{\text{applied}} = 0$ , **b**  $P_{\text{applied}} = 6.897$  kPa using red-color dyed DI water solution, **c**  $P_{\text{applied}} = 0$ , **d**  $P_{\text{applied}} = 68.97$  kPa using DI water



**Acknowledgment** This work was supported in part by the Defense Advanced Research Project Agency (DARPA) under the grant F30602-00-1-0569. The support of University of Texas at Dallas clean room staff and the Micro and Nanotechnology Laboratory of the University of Illinois staff for the fabrication and testing of devices, respectively, is acknowledged.

## References

- Ahn C, Choi J, Beaucage G, Nevin J, Lee J, Puntambekar A, Lee J (2004) Disposable smart lab-on-a-chip for point-of-care clinical diagnostics. *Proc IEEE* 92:154–173
- Davis S, Prausnitz M, Allen M (2003) Fabrication and characterization of laser micromachined hollow microneedles. *Dig. In: Transducers'03, international conference on solid-state sensors and actuators*, pp 1435–1438
- Gardeniers H, Luttge R, Berenschot E, de Boer M, Yeshurun S, Hefetz M, Oever R, Berg A (2003) Silicon micromachined hollow microneedles for transdermal liquid transport. *J Microelectromech Syst* 12:855–862
- Griss P, Stemme G (2003) Side-opened out-of-plane microneedles for microfluidic transdermal liquid transfer. *J Microelectromech Syst* 12:296–301
- Henry S, McAllister D, Allen M, Prausnitz M (1998) Microfabricated microneedles: a novel approach to transdermal drug delivery. *J Pharm Sci* 87:922–925
- Kim K, Park D, Lu H, Che W, Kim K, Lee J, Ahn C (2004) A tapered hollow metallic microneedle array using backside exposure of SU-8. *J Micromech Microeng* 14:597–603
- Lorentz H, Despont M, Fahrni N, LaBlance N, Renaud P, Vettiger P (1997) SU-8: a low-cost negative resist for MEMS. *J Micromech Microeng* 7:121–124
- Lorentz H, Despont M, Fahrni N, LaBlance N, Renaud P, Vettiger P (1998) High-aspect-ratio, ultrathick, negative-tone near-UV photoresist and its applications for MEMS. *Sensors and Actuators A* 64:33–39
- McAllister D, Cros F, Davis S, Matta L, Prausnitz M, Allen M (1999) Three-dimensional hollow microneedle and microtube arrays. *Dig. In: Transducers'99, international conference on solid-state sensors and actuators*, pp 1098–1101
- Moon S, Lee S (2005) A novel fabrication method of a microneedle array using inclined deep x-ray exposure. *J Micromech Microeng* 15:903–911
- Peterman M, Huie P, Bloom D, Fishman H (2003) Building thick photoresist structures from the bottom up. *J Micromech Microeng* 13:380–382
- Stoeber B, Liepmann D (2005) Arrays of hollow out-of-plane microneedles for drug delivery. *J Microelectromech Syst* 14:472–479
- Zhang J, Tan K, Hong G, Yang L, Gong H (2001) Polymerization optimization of SU-8 photoresist and its applications in microfluidic systems and MEMS. *J Micromech Microeng* 11:20–26
- Zimmermann S, Fienbork D, Flounders A, Liepmann D (2004) In-device enzyme immobilization: wafer-level fabrication of an integrated glucose sensor. *Sensors Actuat B* 99:163–173